

MAPPING OF AQUIFER UNITS IN A COMPLEX GEOLOGIC TERRAIN USING NATURAL ELECTRIC FIELD AND ELECTRICAL RESISTIVITY TECHNIQUES

Alabi, A. A.^{1,*}, Ganiyu, S. A.¹, Idowu, O. A.², Ogabi, A. F.¹, Popoola, O. I.³ and Coker, J. O.⁴

¹Department of Physics, Federal University of Agriculture, Abeokuta, Nigeria

²Department of Water Resources Management and Agricultural Meteorology, Federal University of Agriculture, Abeokuta, Nigeria

³Department of Physics, University of Ibadan, Ibadan, Nigeria

⁴Department of Physics, Olabisi Onabanjo University, Ago Iwoye, Ogun State, Nigeria

*Corresponding Author Email: derylab@yahoo.com

(Received: 1st December, 2021; Accepted: 20th September, 2022)

ABSTRACT

Aquifer mapping in a typical complex geologic terrain like Kobape, Southwestern Nigeria is essential to meet the needs of freshwater for domestic and industrial purposes. Natural Electric Field (NEF) measurements over eight traverses and Vertical Electrical Sounding (VES) at ten points were carried out for aquifer mapping in the area. PQWT-TC150 model of a typical water detector, which works by integrating the principle of nuclear magnetic resonance, magnetotelluric and induced polarization methods is used for the NEF measurement. It images the subsurface to a depth of 150 m while the VES was carried out to show the geoelectric layers. The results of NEF revealed the presence of confined aquifer units while the VES showed the subsurface structure to be of 3 to 4 layers viz: topsoil, sandstone, fractured layer, and fresh basement. The corresponding resistivity ranges of the geoelectric layers are 341–3596 Ωm , 1378–4333 Ωm , 635–1000 Ωm , and 3721–56382 Ωm while their thicknesses ranged from 0.5–1.6 m, 0.8–25.4 m, 2.2–19.8 m, and undeterminable fresh basement. The overall aquifer mapping in the complex geologic terrain that straddles the boundary of crystalline basement rocks and a sedimentary basin using integrated technique of NEF and VES revealed various confined aquifers. The NEF significantly showed station twenty on traverse three has a good aquifer within a fractured zone at a depth of 15 m and the same region is verified by the result obtained at VES 3, which has a fractured layer of 19.8 m thickness.

Keywords: Groundwater potential, Confined Aquifer, Natural Electric field, Resistivity, PQWT.

INTRODUCTION

Groundwater contributes substantially to meeting the domestic and industrial needs of the populace across the world and a thorough geophysical investigation is required to validate its availability and accessibility at any point of reference. Its quality can largely be improved by natural barriers and most importantly, very minor treatment can be employed to make it potable (Filimonau and Barth, 2016). Groundwater exists in a geological formation consisting of permeable material like pore spaces, sediments, and fractures in rocks beneath the surface of the earth. Naturally, groundwater recharge can be enhanced by water that leaks through the bottom of some lakes, rivers, rainwater, or via adjacent hydraulic boundaries. The water supply system for irrigation purposes can also contribute to recharging groundwater. There also exist some other techniques to manage aquifer recharge and increase the quantity of water infiltrating into the

ground (Delleur, 2006). The physical characteristics of the region under study, the meteorological conditions, groundwater recharge, and the exploitation rates are parts of the factors that determine whether the water table lies deep or shallow in the subsurface (Muhammad *et. al.*, 2020). Heavy rains likewise have a greater effect to increase aquifer recharge and cause the water table to rise considerably (Delleur, 2006). In addition, an extended period of dry weather may also cause a fall on the water table (Delleur, 2006). For an aquifer to be able to store and yield groundwater, it needs to have empty pore spaces or fractures where groundwater can be stored and the spaces need to be connected to allow it to flow through. Geologically, when connected empty spaces exist in the ground, the geological formation is said to be permeable (Nelson, 2015). On the other hand, the geological formation becomes impermeable when there are no pore spaces or when they are not interconnected. The greater the aquifer's

porosity and permeability, the more groundwater is stored and yielded by the aquifer (Wright, 1992). Consequently, groundwater is observed to be in constant motion, although the rate of transition is generally not like what is observed in a stream because it passes through the free spaces in the surrounding rocks. The pull of gravity causes groundwater to naturally move downward, however, water flow capacity can make groundwater move upward from a region with higher pressure to a region with lower pressure (Guru *et al.*, 2017; William *et al.*, 2002).

The combination of Vertical Electrical Sounding with the electromagnetic method of geophysical investigation has been used for groundwater investigation in different basement complex terrain (Afolayan *et al.*, 2004; Sharma and Baranwal, 2005; Alabi *et al.*, 2020). Onoja and Osifila (2015) applied integrated geophysical techniques involving self-potential, electrical resistivity, and electromagnetic methods to study the nature of the spring in Igbokoran, Ikare Akoko, Ondo State, Nigeria. The combined results revealed three geoelectric layers with the suspected fractured basement along the third traverse. The groundwater feasibility study was also carried out around the suspected spring and confirmed that it has a low groundwater yield due to the thin overburden and the low fracture density of the basement. Parasnis (1997) submitted that large data sets using deep VES and time-domain electromagnetic methods are required for better analysis of aquifer units. Oyegoke *et al.* (2020) employed PQWT instrument to evaluate the effectiveness of boreholes drilled in basement complex terrain at Afe Babalola University. It was noted that the instrument is easy to operate with little or no field experience, and it can generate a 2D image of the subsurface at a go for quick groundwater detection. Ranganai *et al.* (2018) also used PQWT instrument for magnetotelluric method in integrated geophysical methods to decipher hydrogeological characteristics of a groundwater borehole site in the University of Botswana Gaborone. The results confirmed the importance of a systematic geoscience approach to locate the best drilling site/location for a successful borehole. Oladele and Odubote (2017) combined geophysical logs with VES in the mapping and

characterization of aquifer units in Ijebu Ode, Southwestern Nigeria. The site was suspected to be a typical complex transition zone and the investigation was done to appraise the groundwater potential of the area. The VES survey was done using the Schlumberger array method over a current electrode spacing of 900 m at sixteen points. Electric logging that involves the measurement of natural gamma rays was used to acquire the resistivity of the area under investigation. Four geoelectric layers were revealed from the processing of the sounding data and the fractured layer was observed at 80 m below the surface. It was concluded that the study area which lies in a complex transition zone has a low prospect for groundwater exploration (Olayinka *et al.*, 2004). Successful exploration of groundwater in a typical complex geologic terrain like Kobape requires a proper understanding of the geo-hydrological characteristics of the aquifer units with their environmental susceptibility (Abiola *et al.*, 2009). This is due to the localized discontinuous nature of the basement aquifers. This research was aimed at locating suitable zones for groundwater exploration and determining the depth of sustainable groundwater occurrence in Kobape, a transition zone.

Site Description and Geological Setting

The study area is located in Kobape, Southwestern Nigeria, and lies between latitude 7° 3' 18"N to 7° 3' 25" and longitude 3° 30' 40"E to 3° 30' 41"E. The ground elevation varies between 169–186 m above sea level while the mean annual rainfall, mean annual potential evaporation, and temperature of Abeokuta are 1238 mm, 1100 mm, and 27.1 °C respectively (Akinse and Gbadebo, 2016). The study area has a tropical savanna climate with the wet season having a good deal of rainfall and very little in the dry season. The rainy season in the area commences in March and subsides in October while the dry season usually surfaces from November to February under the influence of North-Easterly winds from the Sahara Desert (Badmus and Olatinsu, 2010).

The geology of Nigeria consists of two broad geological terrains, which are basement complex and sedimentary terrain according to Obaje (2009). The basement complex terrain consists of crystalline igneous and metamorphic rocks which

can either be found on the surface or covered by a shallow mantle of superficial deposits in some areas (Adeeko and Ojo, 2015). The crystalline basement rocks that occur in Nigeria have been broadly classified into five major lithological groups namely; Magmatic-gneiss complex, Metasedimentary and metavolcanic rocks, Charnockitic rocks, Older granite, Unmetamorphosed dolerite dykes (Obaje, 2009). The Sedimentary rocks, on the other hand, occur in seven basins which are in the northeast (Chad basin), northwest (Sokoto basin), southwest (Dahomey basin), Niger, Anambra, Niger Delta, and the Benue Trough (Avbovbo, 1980). The geologic formation in Ogun state and that of the area under investigation are shown in Figure 1. The area is made up of three main formations,

namely: Ise formation, Afowo formation, and Araromi formation (Omatsola and Adegoke, 1981; Mosuro *et al.*, 2011). The physical outcrops sighted around the area are quartz-mica schist and migmatite-gneiss to a lesser extent. The quartz-mica schist consists of muscovite, biotite, quartz, and feldspar while the mineral constituents of migmatite-gneiss in order of abundance are quartz, biotite, muscovite, and feldspar from the field observation (Rahman, 1989; Caby, 1989; Ariyo and Adeyemi, 2012). The area under investigation is situated in between the basement complex group of Abeokuta and sedimentary terrain Sagamu. Coker *et al.* (2014) reported that the terrain where the study area falls is a suspected transition zone.

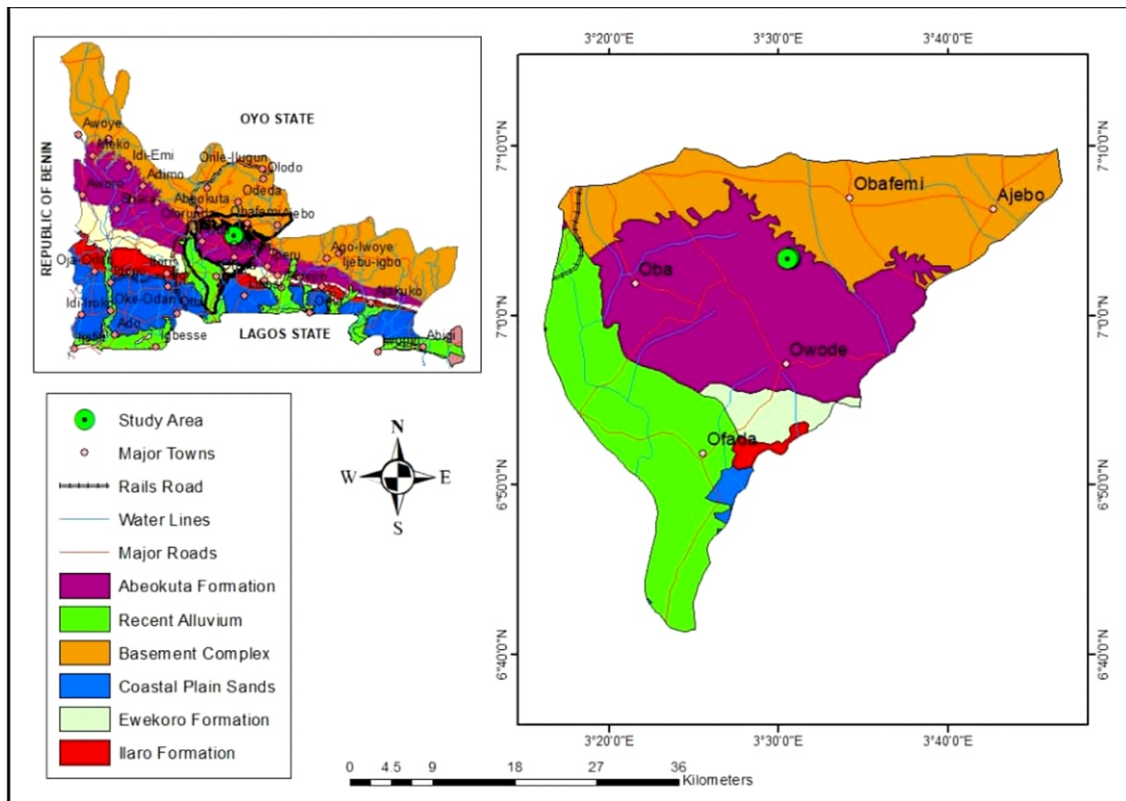


Figure 1: Geological Map of Ogun State showing Obafemi Owode Area.

METHODOLOGY

Natural Electric Field (NEF) method

The natural electric field measurement in the study area was carried out with a new geophysical exploration instrument called PQTW. The model of the device used in this research work is PQWT-TC150 and it is one of the latest groundwater detectors manufactured by Hunan Puqi Geologic Exploration Equipment Institute, China. The instrument is also referred to as a natural electric field frequency selection system because it uses the natural electric field as the field source (Hunan, 2017). PQWT-TC150 operates based on the differences in the conductivity properties of the underground geological structures. It measures the electrical difference of natural earth magnetic field and their variation at different frequencies and depths. The principle of nuclear magnetic resonance (NMR), magnetotelluric and induced polarization are the three integrated geophysical methods that PQWT technology is based upon to find subsurface water resources and geological ore deposits (Heilig *et al.*, 2018). The performance of NMR depends on the magnitude of the natural geomagnetic field, the electrical conductivity of rocks, and the electromagnetic noise. The earth's steady magnetic field is produced by many sources, both above and below the planet's surface (Hunan, 2017). The primary source of the field is the self-sustaining geodynamo action of the Earth's liquid outer core. The geomagnetic dynamo happens to be the most important natural field source because all other sources depend on it. In the dynamo mechanism, fluid motion in the core moves conducting material across an existing magnetic field and creates an electric current. This current produces a magnetic field that also

interacts with the fluid motion to create a secondary magnetic field with the same orientation as the original field (Heilig *et al.*, 2018).

PQWT adopts a physical phenomenon where nuclei in a strong constant magnetic field are perturbed by a weak oscillating magnetic field and respond by producing an electromagnetic signal with a frequency characteristic of the magnetic field at the nucleus (Legchenko, 2002). This process occurs near resonance when the oscillation frequency matches the intrinsic frequency of the nuclei. This however depends on the strength of the static magnetic field, the chemical environment, and the magnetic properties of the isotope involved (Legchenko *et al.*, 2002). Conventionally, radiations from the earth that originates from the rock minerals, ore bodies, subsurface water, or other geological structures are affected by a magnetic or electric field and when these radioactive emissions pass through a magnetic field or charged plates they disintegrate into alpha particles, beta particles, and gamma rays (Figure 2). The Gamma rays are electromagnetic waves with no charge, and it remains un-deflected through the field. This is the phenomenon that produces the natural electromagnetic field whose electric field component can be measured to determine the resistivity properties of the originating material in the subsurface. The variations in the frequencies of the electromagnetic field in the subsurface, ranging from 0-30 KHz thus incorporated by PQWT-TC150 to study the underground field to solve imposing geological problems (Harinath, 2020).

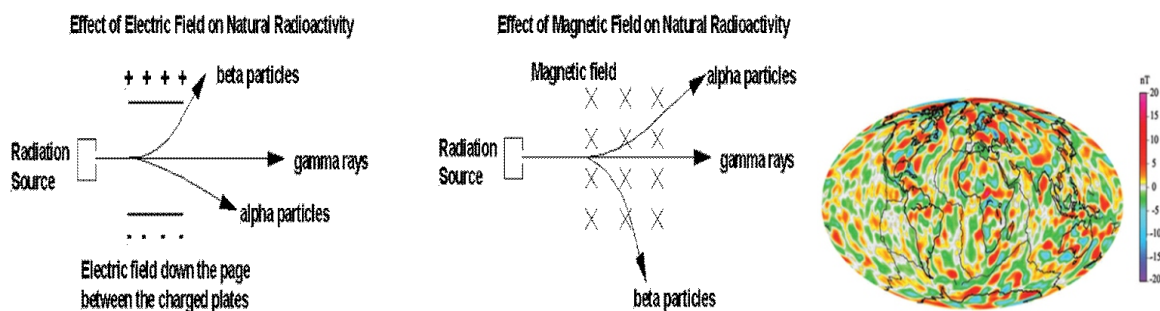


Figure 2: The effect of Magnetic and Electric Fields on Natural Radioactivity (Frey, 2011).

The NEF survey by PQWT-TC150 involves the passive measurement of the electric E and the magnetic B fields in an orthogonal direction at the ground surface of the earth with two non-polarizable potential electrodes. The geomagnetic field is regarded as a plane wave whose distribution is perpendicular to the ground and is distributed far from the field source. The ratio of the horizontal electric, and the magnitudes of the magnetic field (e.g. E_x and H_y) are measured in the time/frequency domain and are used to calculate the resistivity structure of the earth by the PQWT instrument. The apparent resistivity of the medium under interaction is derived by substituting electric and magnetic field components in Cagniard's scalar resistivity formulae to give equation 1 (Cagniard, 1953; Waff, 2000).

$$\rho_m = \frac{1}{5f} \left(\frac{E_x}{H_y} \right)^2 \quad (1)$$

where ρ_m is the resistivity of the medium under interaction, f is the operating frequency, H_y and E_x are the magnetic field and electric field components of the field, respectively. The electric field component of the field interacts perpendicularly to the ground while the magnetic component of the field is taken to be constant. Hence the qualitative relationship between the electric field component and the resistivity of the ground under interaction can be used to determine the geologic characteristics of the material under interaction. The depth of penetration (δ) of a plane electromagnetic waves propagated on the ground according to attenuation characteristics is given in equation 2, and it implies that the penetrating depth of electromagnetic waves in a medium is directly proportional to the resistivity of the media at a constant frequency.

$$\delta = 503.3 \sqrt{\frac{\rho}{f}} \quad (2)$$

Equation 2 can then be used to transform equation 1 into a one-dimensional depth inversion with the assumption that the 1D slice is an artificial representation of the earth with equal impedance and using the Maxwell electromagnetic theory with the assumption that the ground is homogeneous, isotropic, and horizontally layered. The effects of the

displacement current where E_x and H_y fall between the $\frac{\pi}{2}$ phase angle are likewise ignored, meaning that the data collection lines are perpendicular to the structure (Rensburg, 2019). The premise on which magnetotellurics procedure is part of the PQWT-TC150 operation is because the magnetic field is stable in most scenarios and it is regarded as a constant function of the electric field response over a small area of measurement (Zonge and Hughes, 1991)

The field measurement was done by placing the two potential electrodes at points N and M; 10 m apart on the ground to take the first reading on each traverse. A console cable was used to connect the probes to the instrument which determines the electromagnetic impulse generated by those points and the data generated are saved automatically on the instrument. The N and M electrodes were consequently moved 5 m progressively on the traverse line, that is N is moved to 5 m, while M is moved to 15 m to take the next reading (Figure 3). These processes were thus followed until the entire length of the transverse is completed. The electrical potential differences between the pairs of electrodes that contact the ground are the primary data captured at the selected 21 different stations on each of the eight traverses in the study area. The instrument at a push of a button measures the electric field component of thirty-six different frequencies in the geomagnetic field in millivolt (mV) and a frequency curve with a profile map is generated on the display of the PQWT-TC150. The frequency curve displayed how the normal frequency lines within the subsurface respond to the application of a small potential difference in millivolt by the instrument (Hunan, 2017). A straight frequency line reveals a homogenous subsurface material while a curvy or angular line indicates variations in rock properties. The algorithm on the PQWT-TC150 is computed with equations 1 and 2 to use the electric field response in mV to generate a profile map with a resistance bar usually shown at the right-hand side of the map from red at the top to blue at the base (Kearey, 2002; Hunan, 2017). The regions with a red colour scheme indicate the highly resistive zones, and as the colour spectrum migrates towards the blue colour the resistance diminishes. Regions with a high tendency for

groundwater are identified with a bluer colour concentration on the profile map while fractures

and faults are noticeable where typical contour lines concentrate (Hunan, 2017 and Hunan, 2018).

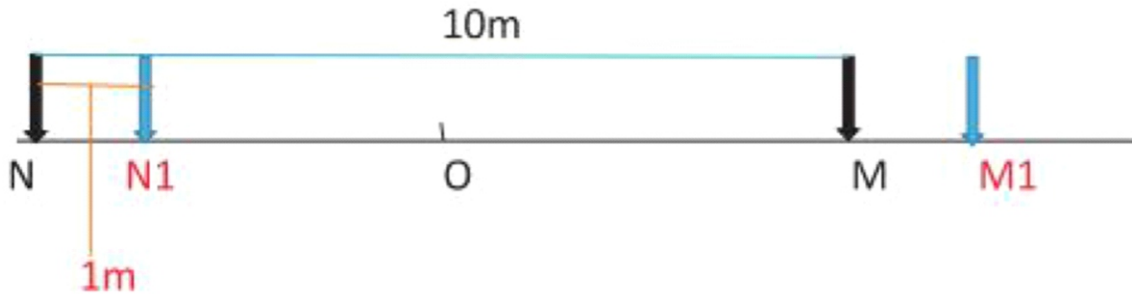


Figure 3: PQWT Instrument setup and electrode arrangement.

Vertical Electrical Sounding Method

The VES survey was carried out over a half-current electrode spread (AB/2) of 100 m. The current sounded at points A, and B develops a ground potential difference whose voltage was determined by another two electrodes that are kept in line with the pair of current electrodes at points M and N. The resistivity meter generates the resistance of the materials underneath the sounding points and when multiplied with the corresponding geometric factor the apparent resistivity is obtained. The apparent resistivity is measured in Ohmmeter (Ωm) and it is required during interpretation. Apparent Resistivity (ρ_a) is the product of the geometric factor (G) and the measured resistance (R). The required apparent resistivity (ρ_a) results as functions of depths of individual layers given as:

$$\rho_a = \pi R \left(\frac{L^2 - l^2}{2l} \right) \tag{3}$$

Where: ρ_a is Apparent Resistivity for Schlumberger array; R is Resistance in ohms; L/2 is current electrode spacing (m); l/2 is potential electrode spacing (m).

$$G = \pi \left(\frac{L^2 - l^2}{2l} \right) \tag{4}$$

The VES resistivity data obtained on the field were partially curve matched before being computer iterated with WINRESIST software with an R.M.S error of less than 5.0 to obtain the true resistivity and layer parameters (Van der Velpen,

2004). The iterated geoelectric parameters obtained were used to generate geoelectric sections.

RESULTS AND DISCUSSIONS

NEF Results and Interpretation

In the Natural Electric Field measurements, an average of 21 readings were taken at 5 m sampling intervals on each of the 8 selected traverses. The generated frequency curve is a plot of thirty-six frequency responses of the earth's electromagnetic field in millivolt (mV) on the vertical axis and the lateral sampling distance on the horizontal axis. The corresponding profile maps provide the pictorial interpretation of the frequency response of the subsurface to a depth of 150 m. The vertical axis shows the depth into the subsurface and the horizontal axis gives the lateral distance covered. The frequency response is used to map the contour lines on the profile map and the regions where the lines concentrate or diverge reveal the presence of a significant anomaly.

The frequency curve from traverse 1 has a peak potential response of 36.6 mV on the eighth measurement along the traverse. The normal frequency lines show some distinct curvy responses at stations 3-5 and across the whole length of the profile. These curvy responses are in turn interpreted on the profile map as a vertical fracture between stations 2 to 5 (10 to 25 m) along the traverse at a depth of 40 to 130 m and another

concentrated fractures at stations 11 to 14 (55 to 70 m) and at 16 to 19 (80 to 95 m). The top layer of this traverse is observed to be fractured up to about 20 m below the surface, and it is underlain by another lower resistive layer up to about 60 m

below the surface. The rest of the subsurface from 60 m to where the investigation covered has a moderate resistance property with varying concentrations of contour lines (Figure 4).

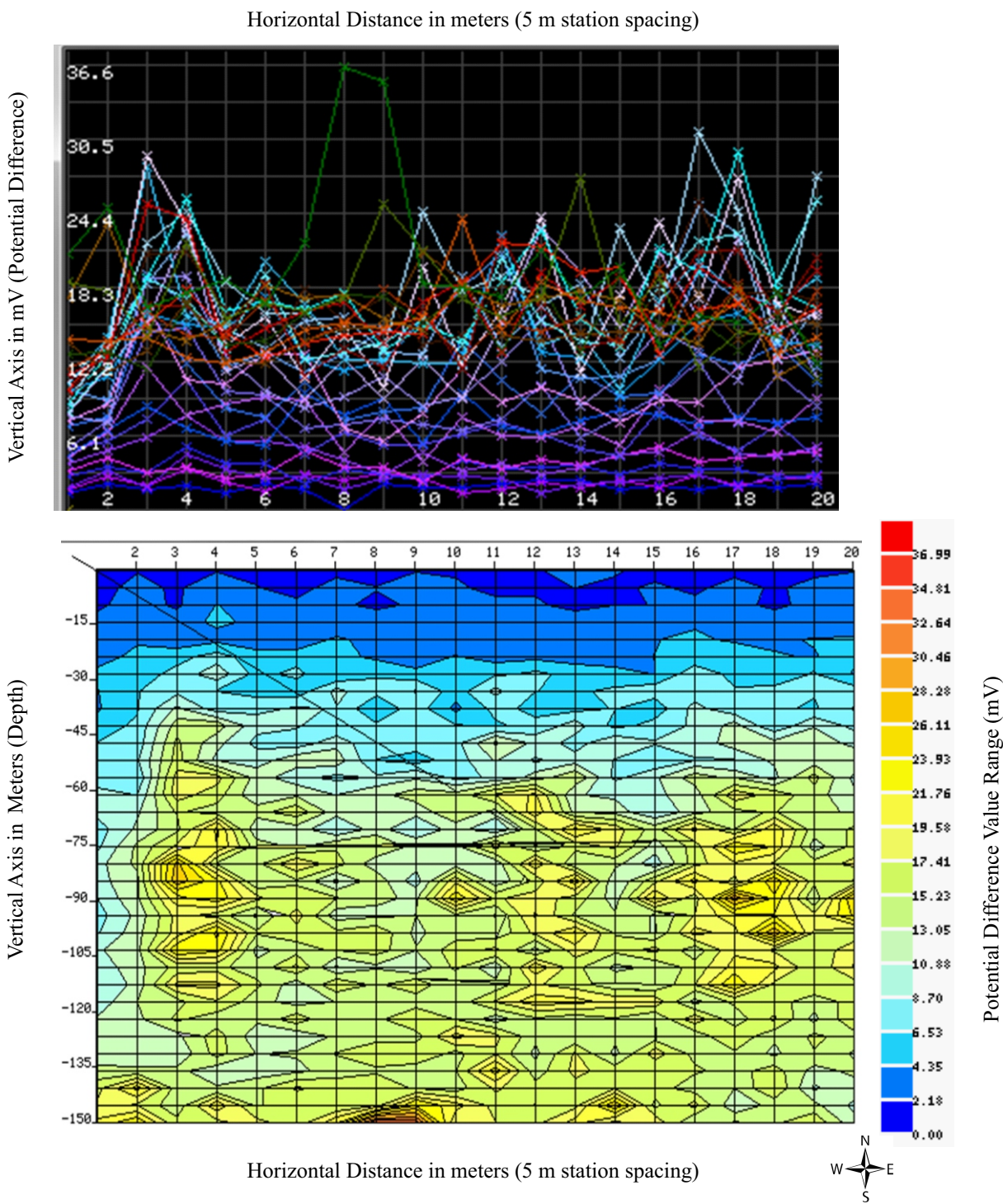


Figure 4: Frequency Curve and profile Map for Traverse 1.

The second traverse has a peak potential response of 4.9 mV at station 19 of the traverse with other sharp variations of about 2.05 mV at stations 13 and 16. These responses were interpreted on the profile map as a vertical fracture centered at station 18 (90 m) between the depth of 75 and 90 m from the ground surface. A highly resistive body was observed at a depth of 130 m into the subsurface at the same station (Figure 5). The top layer on this traverse is also observed to be moderately resistive to an average depth of 30 m from the surface, and it has a pocket contour at station 13 along the profile. Another lower resistance layer underlined the top layer into the subsurface which has a fractured zone between points 3 (15 m) and 6 (30 m) along the traverse at a depth of 75, 110, and 125 m from the ground surface.

A peak potential response of 0.3 mV was observed at station 17 on the third traverse and most of the normal frequency lines showed minimal variation but concentrated around 0.0 and -0.1 mV. The interpreted profile map reveals only two pocket fractures at stations 17 and 20 at a depth of 5 and 85 m below the surface, respectively (Figure 6). The resistance of the media across the profile is inhomogeneous but varies closely at a lower potential value having a moderately

fractured layer at an average depth of 25 to 135 m below the surface.

The frequency curve generated from the fourth traverse measurement has a peak potential response of 0.4 mV at station 11. A distinct variation from the normal frequency lines was observed at stations 2-4, 10-12, and 18-20 and was interpreted on the profile map as another material medium that is fractured (Figure 7). A vertical fracture is noticeable at point 3 (15 m) along the traverse and the region is observed to have a higher potential value in the medium range. An extending fractured zone from points before the starting point of the survey was noticed at an average depth of 70, 105, and 120 to 135 m below the surface around the starting point. Other fractured zones were observed to center at point 10 (50 m) and point 20 (100 m) along the traverse. Scanty fracture zones were likewise noticeable to the center at points 11 (55 m) and 19 (95 m) along the traverse at the depth 90-120 m and 30 m respectively below the surface. There exist other layering variations along the traverse from point 12 (60 m) at the depth of 120 m moving up to the depth of about 20m below the surface at point 18 (90 m) towards the end of the traverse.

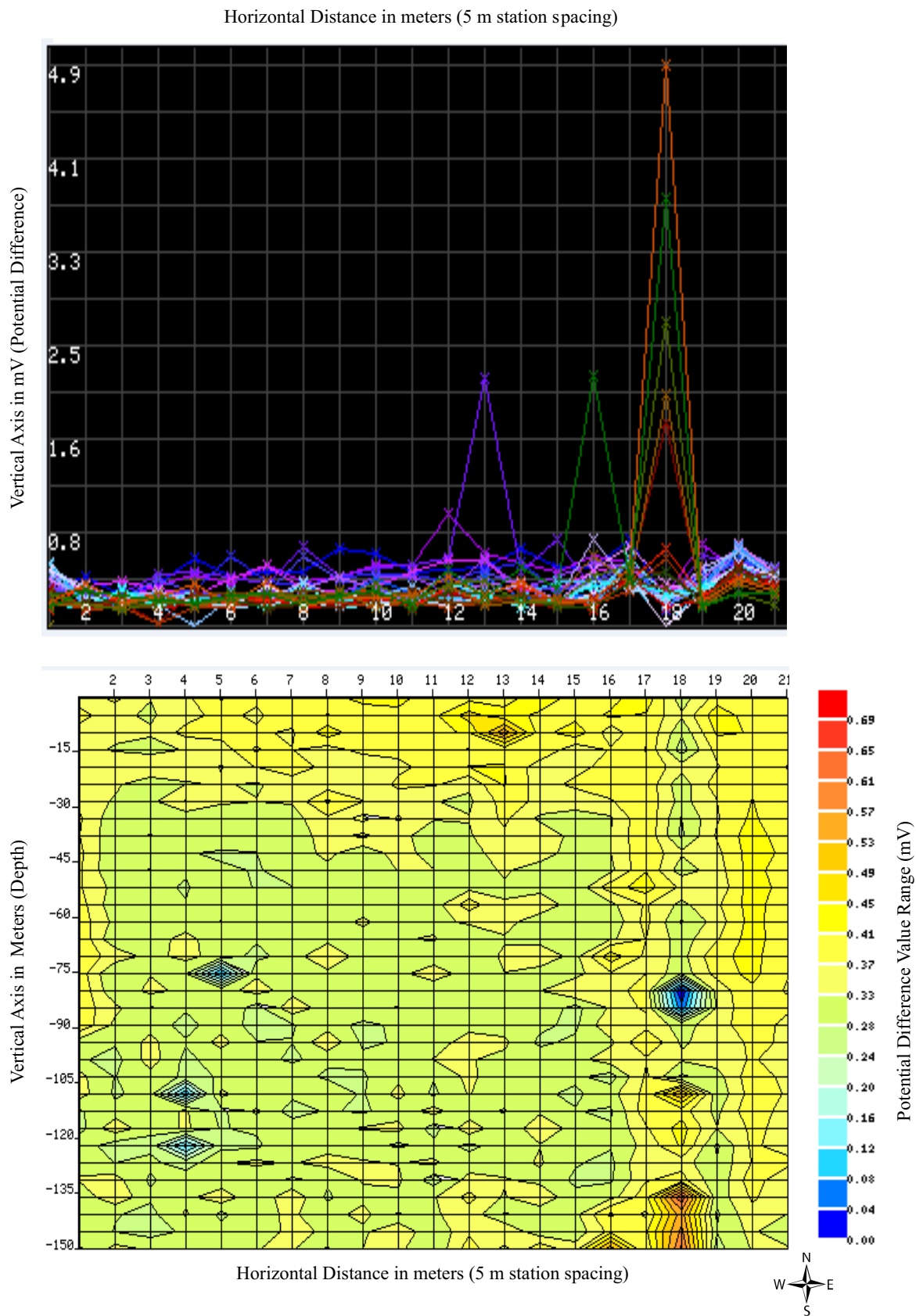
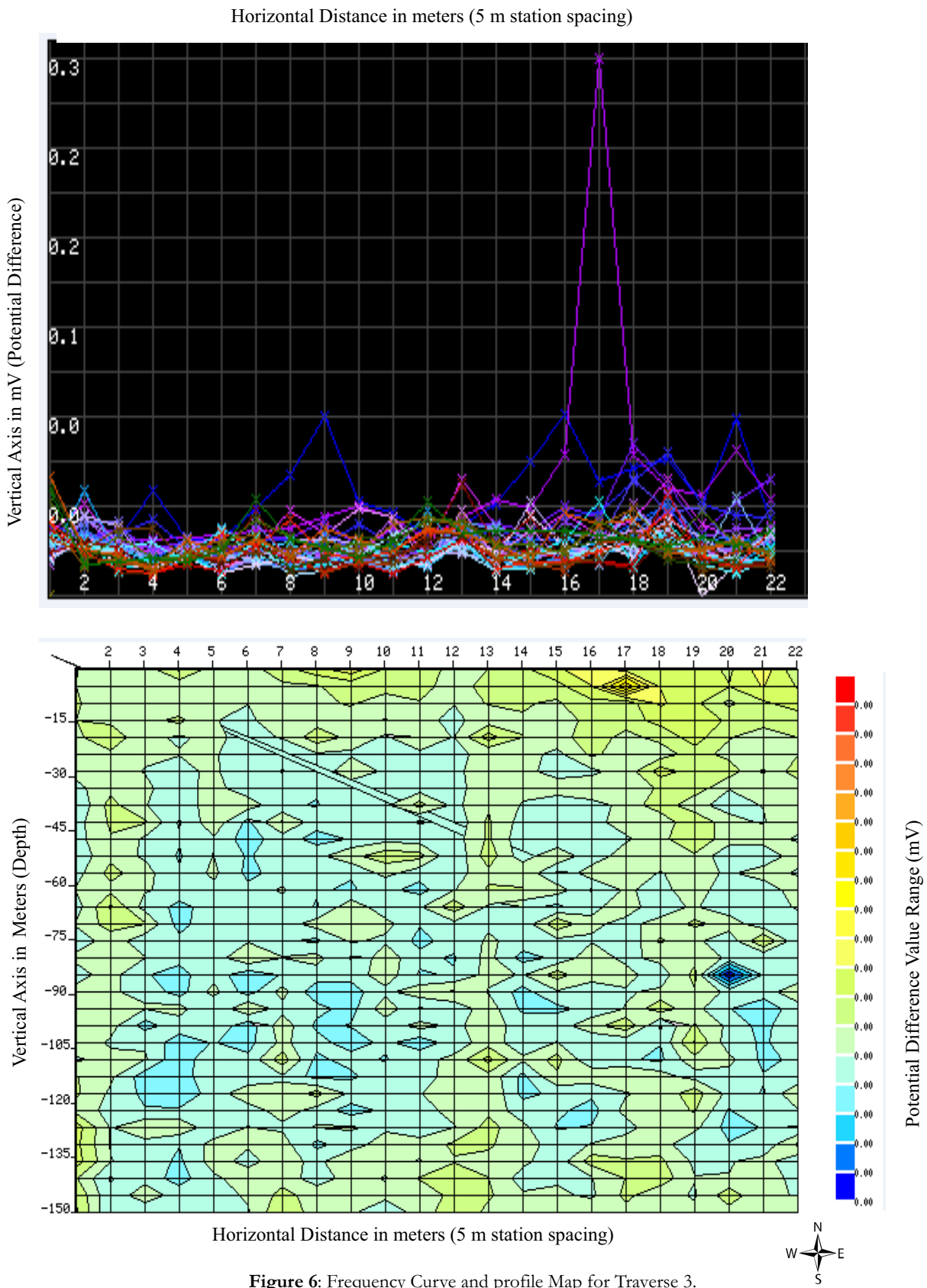


Figure 5: Frequency Curve and profile Map for Traverse 2.



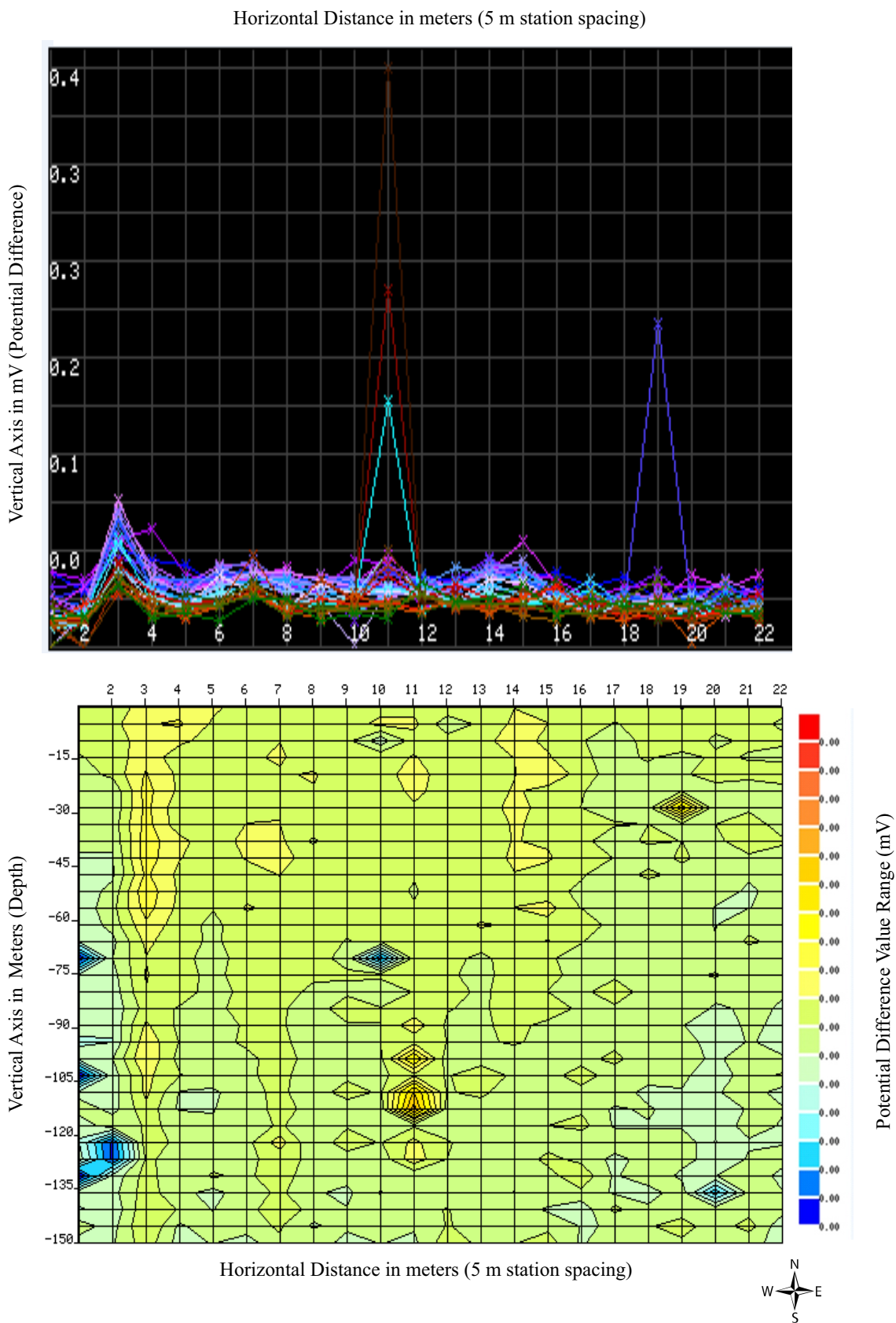


Figure 7: Frequency Curve and profile Map for Traverse 4.

A peak potential response of 8.5 mV was revealed on the fifth traverse at station 11. The normal frequency lines show some distinct curvy responses at stations 6–8, 10–12, and 13–15. The interpreted profile map revealed that the area under investigation has more pronounced vertical material variations (Figure 8). The zones before the profile's starting point show an extending fracture which is immediately followed by a more resistive medium from stations 2 to 5 with an average thickness of 75 m towards the surface. A moderately low resistive vertical fracture is noticeable to center at point 9 from an approximate depth of 70 m and just next to it is a feature of high resistive material that is about 10 m wide and 65 m thick. Other varying fractures with lower resistance are noticeable at stations 18, 19, and 20 at a corresponding depth of 145, 95, and 115 m.

Traverse 6 has a peak potential response of 1.8 mV at station 18. The frequency responses are observed to converge largely between stations 7 and 15 which the interpreted profile map revealed to be a highly resistive region (Figure 9). The top layer is relatively constant on the resistance scale to an average depth of 15 m below the surface and this same material is observed to vertically extend deeper into the subsurface between stations 2 to 5 and at stations 7 to 15 across the profile. Large varying contour lines indicating vertically fractured zones were observed at stations 2–4,

5–7, 15–18, and station 19 towards the end of the traverse. These occur at an average depth of 60 m below the surface and beyond 150 m in all cases.

A peak potential response of 9.1 mV was noticed on traverse 7 at station 13 with very few changes on the normal frequency lines between stations 5–8 and 16–18. The profile map generated from this survey showed that the line under investigation has a uniform lateral resistance variation with traces of vertical anomalies across the traverse (Figure 10). A vertical contour pocket is observed to center at station 13 (65 m) even extending to a rocky outcrop as observed from the field inspection. Other uniform anomalies observed on this profile occur at the beginning of the traverse to around station 3, another from the base of the profile from station 4–8, and towards the end of the profile at station 18.

The frequency curve generated from the eighth traverse has a peak potential response of 3.6 mV at station 21 on the profile (Figure 11). The potential response drops to 0.0 mV at stations 11, 18, and 21 revealing a highly fractured zone with very low resistance. The profile map generated from this traverse shows that the potential of the region from the beginning of the profile to station 8 is higher around 2.6 mV and diminishes from station 8 to 13 around 2.4 mV where further regions become inhomogeneous.

Horizontal Distance in meters (5 m station spacing)

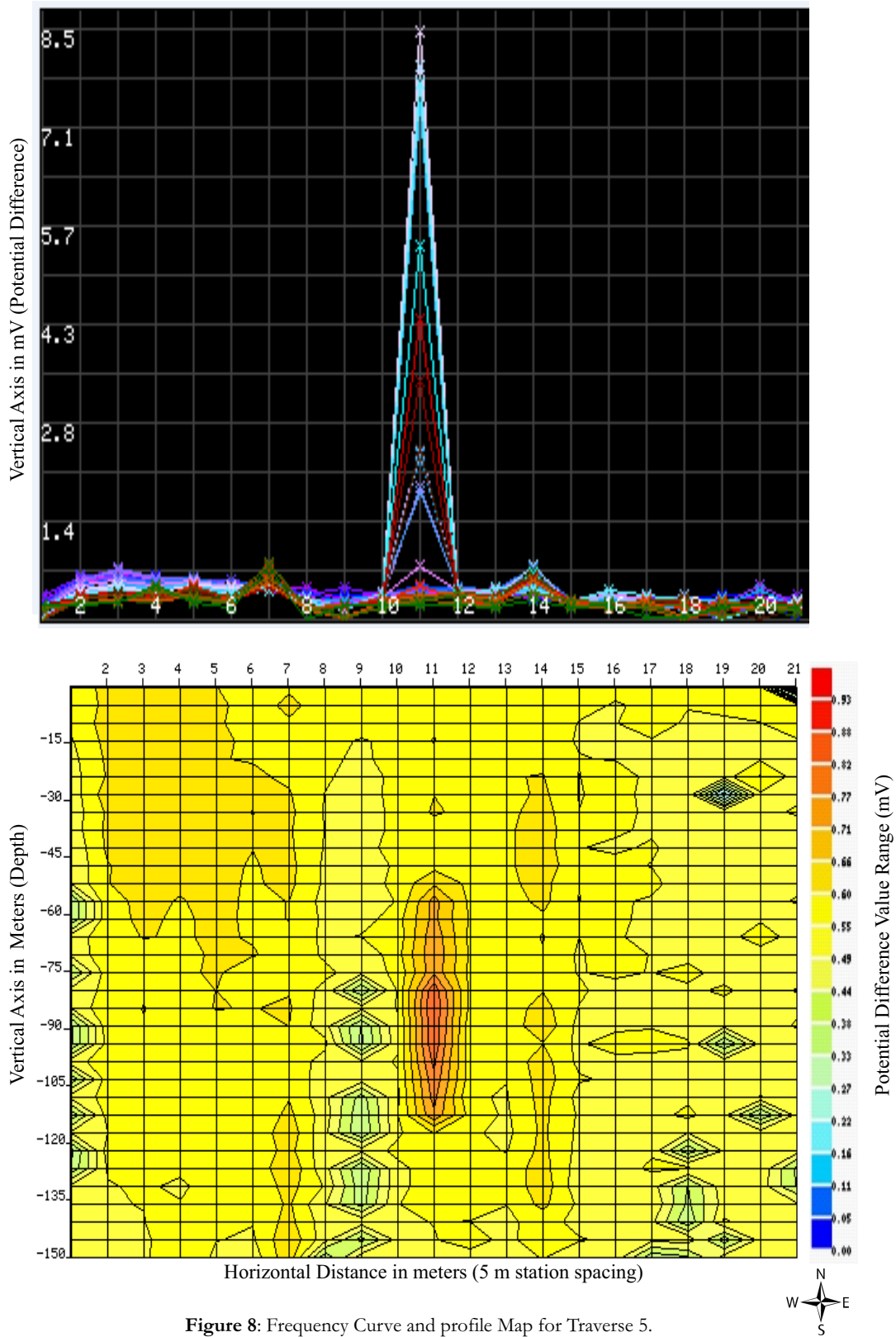


Figure 8: Frequency Curve and profile Map for Traverse 5.

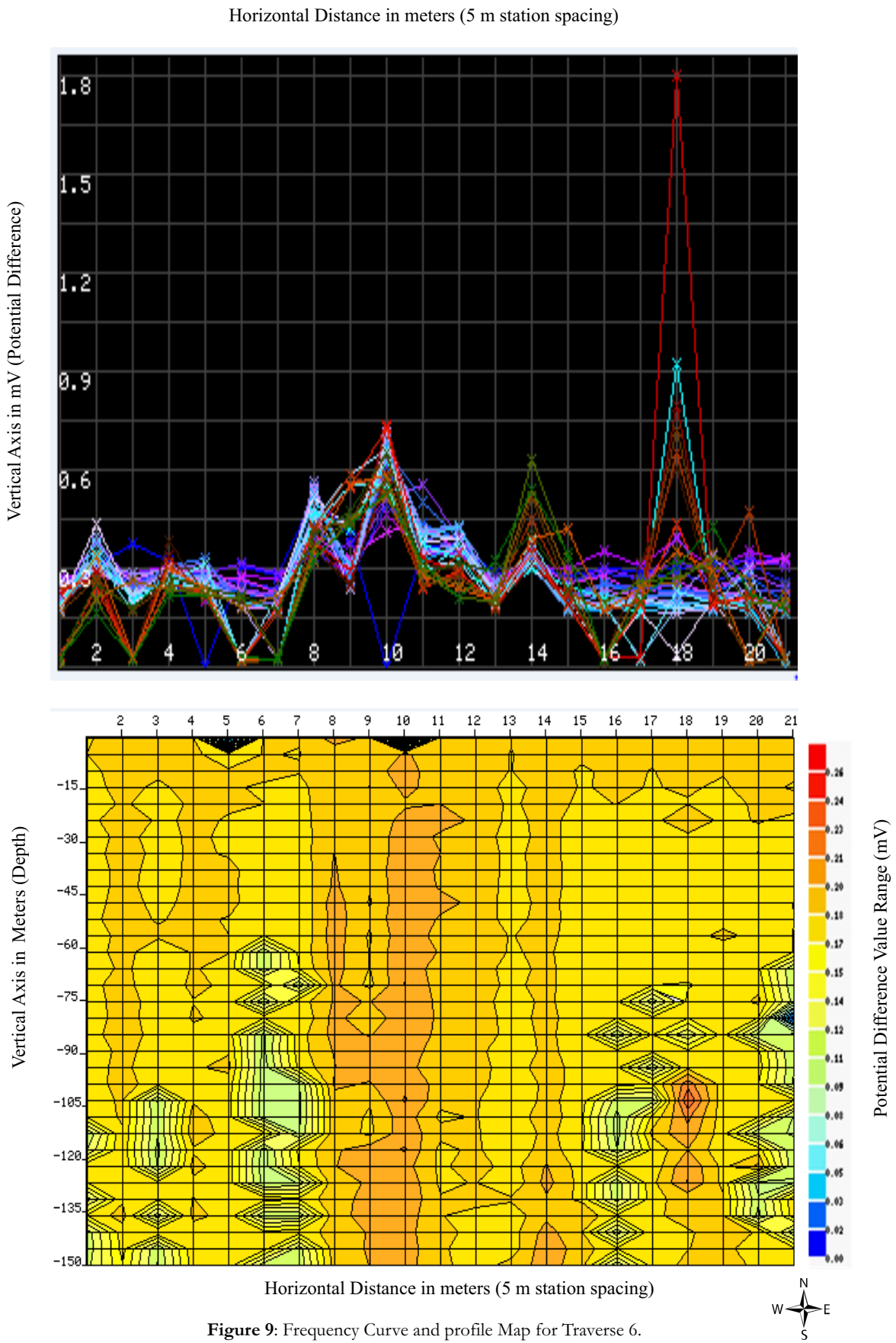


Figure 9: Frequency Curve and profile Map for Traverse 6.

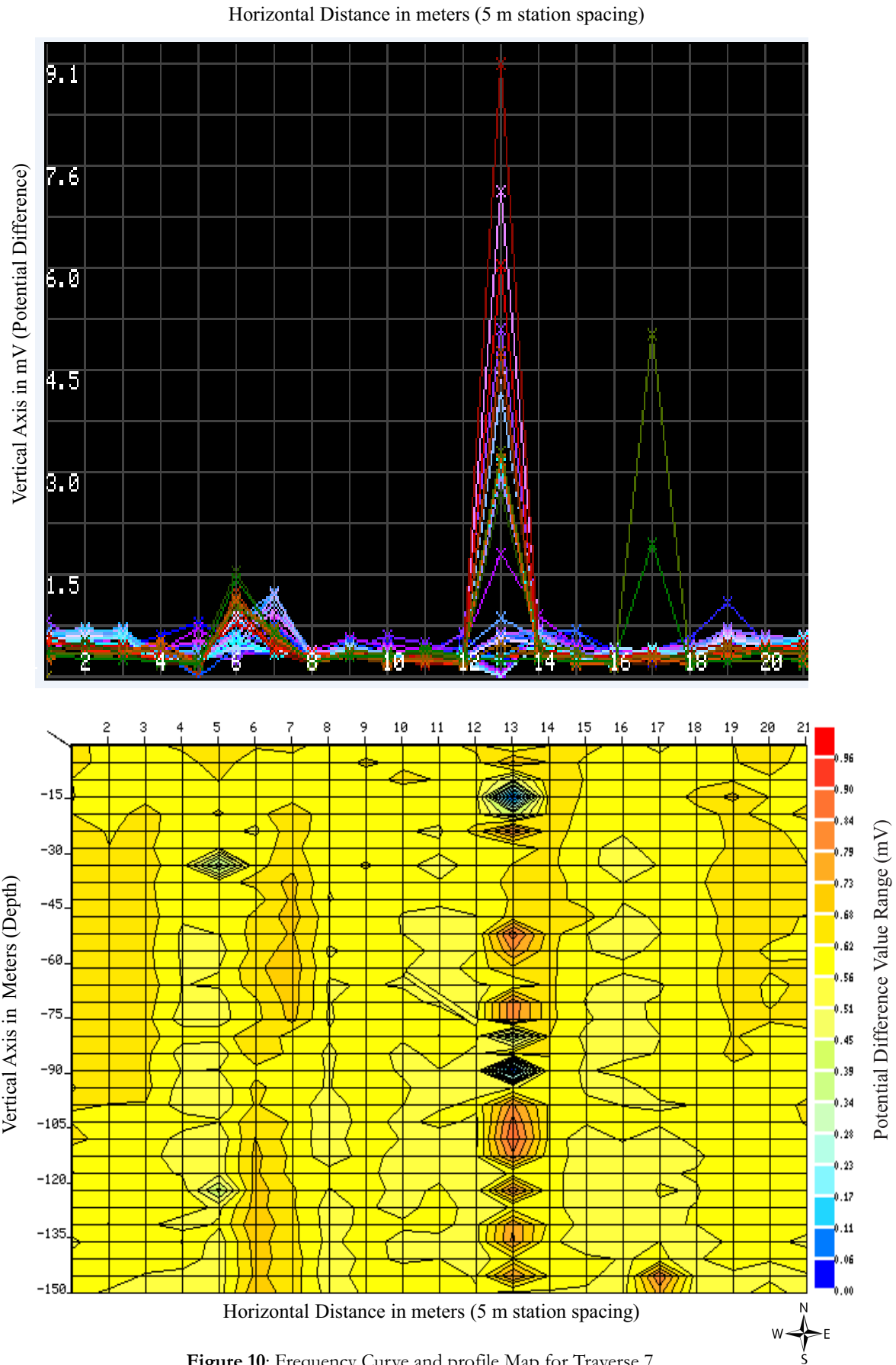


Figure 10: Frequency Curve and profile Map for Traverse 7.

Horizontal Distance in meters (5 m station spacing)

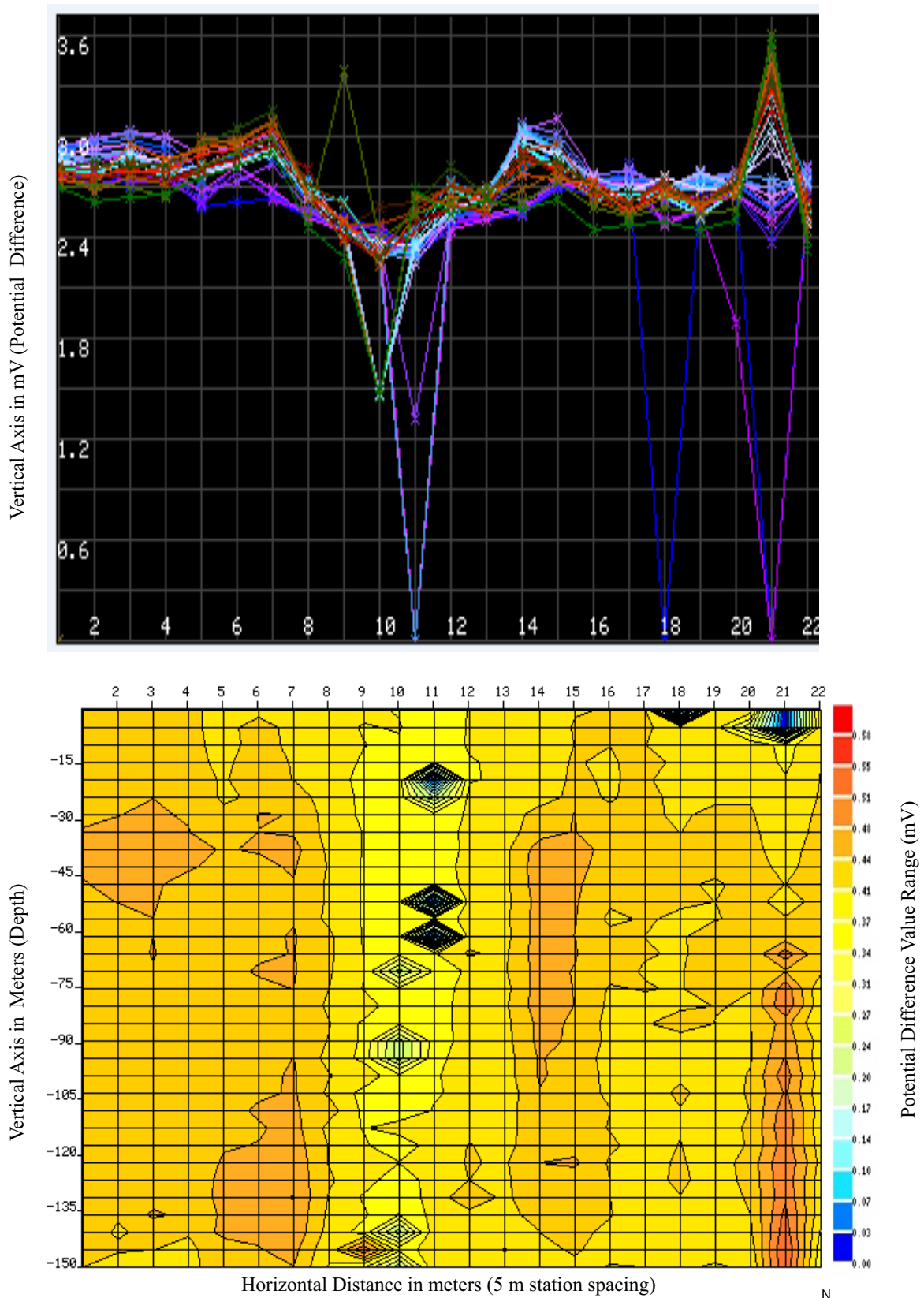


Figure 11: Frequency Curve and profile Map for Traverse 8.



VES results and interpretation

The summary of the geoelectric parameters is shown in Table 1 and the RMS relative error obtained is within the average of 2%. The curve types are classified into four distinct classes: class 1 type curves represent a subsurface condition in which there is an increase in resistivity values from the topsoil to the basement rock as seen in the A-type curves from VES 4 and VES 7 in the survey. Class 2 curve types have the layer underlying the upper horizons when not leached to be of low resistivity and immediately followed by the fresh basement. H-type curve pattern is produced by this architecture and it is typical of what was inferred at VES 3 and VES 8 in the investigation. Curve types of class 3 are typically a succession of relatively low and high resistivity layers. The K-type curves observed at VES 1, VES 5, and VES 6 of the investigation belong to this class as a highly resistive lateritic layer underlies low resistivity topsoil and fractured zone, which in turn, underlies the former. Finally, curve types in class 4 have the succession of the subsurface layers starting with highly resistive topsoil followed by a more conductive horizon, and then another less conductive layer underlies the latter. The curve types inferred from VES 2, VES 9, and VES 10 from the study area are part of this classification.

The sounding responses from points 1, 2, 6, 9, and

10 showed four geoelectric layers with the sandy topsoil above a sandstone layer and followed by the fractured layer to a fresh basement. The resistivity of the topsoil ranges from 564 to 6139 Ωm while that of the fractured layer ranges between 725 and 1000 Ωm with a thickness range of 9.7 to 14.5 m. Three layers were revealed from the sounding curve processing at points 3, 4, 7, and 8 with a resistivity range of 341 to 1735 Ωm for the topsoil and the resistivity of the fractured layer range between 725 and 1000 Ωm . The thicknesses range of the fractured layer ranges between 9.5–26.1 m. Only VES 5 shows a significant difference in the number of geoelectric layers. It has five layers with sandstone of about 68.5 m thickness in between the fractured layer and the fresh basement. The resistivity of the fractured layer at this point is 635 Ωm with a thickness of 3.6 m.

The geoelectric section deduced from the apparent resistivity of each stratified layer with corresponding probed depth is shown in Figure 13 and it is drawn to have a graphical representation of the subsurface geology using the sounding profiles. The section is useful to identify the levels of the water table. The geoelectric section likewise revealed the thickness of the fractured layer to the basement and, it is observed to be on an average scale of 12 m.

Table 1: The geoelectric parameters.

VES No.	No. of Layers	Resistivity (Ωm)	Thickness (m)	Depth (m)	Lithology	Curve Type
1	1	564	0.5	0.5	Topsoil	KH
	2	3592	0.8	1.3	Sandstone	
	3	726	9.0	10.3	Fractured Layer	
	4	17204	-	-	Fresh Basement	
2	1	3596	0.5	0.5	Topsoil	QH
	2	1406	5.8	6.3	Sandstone	
	3	725	5.7	12	Fractured Layer	
	4	27995	-	-	Fresh Basement	
3	1	1448.3	1.6	1.6	Topsoil	H
	2	859.5	19.8	21.4	Fractured Layer	
	3	56382.1	-	-	Fresh Basement	
4	1	1179	0.71	0.71	Topsoil	A
	2	1753	25.4	26.1	Sandstone	
	3	10285	-	-	Fresh Basement	
5	1	1241	0.5	0.5	Topsoil	KHKA
	2	4333	0.8	1.3	Sandstone	
	3	635	2.2	3.6	Fractured Layer	
	4	4829	64.9	68.5	Sandstone	
	5	12679	-	-	Fresh Basement	
6	1	825	0.5	0.5	Topsoil	KH
	2	1378	0.8	1.3	Sandstone	
	3	972	8.4	9.7	Fractured Layer	
	4	6608	-	-	Fresh Basement	
7	1	341	0.6	0.6	Topsoil	A
	2	882	13.2	13.8	Fractured Layer	
	3	30043	-	-	Fresh Basement	
8	1	1735	0.5	0.5	Topsoil	H
	2	907	9.0	9.5	Fractured Layer	
	3	4576	-	-	Fresh Basement	
9	1	6139	0.5	0.5	Topsoil	QH
	2	2021	1.7	2.2	Sandstone	
	3	1000	9.8	12.1	Fractured Layer	
	4	5539	-	-	Fresh Basement	
10	1	1092	0.5	0.5	Topsoil	HA
	2	472	1.9	2.4	Sand	
	3	804	12.1	14.5	Fractured Layer	
	4	3721	-	-	Fresh Basement	

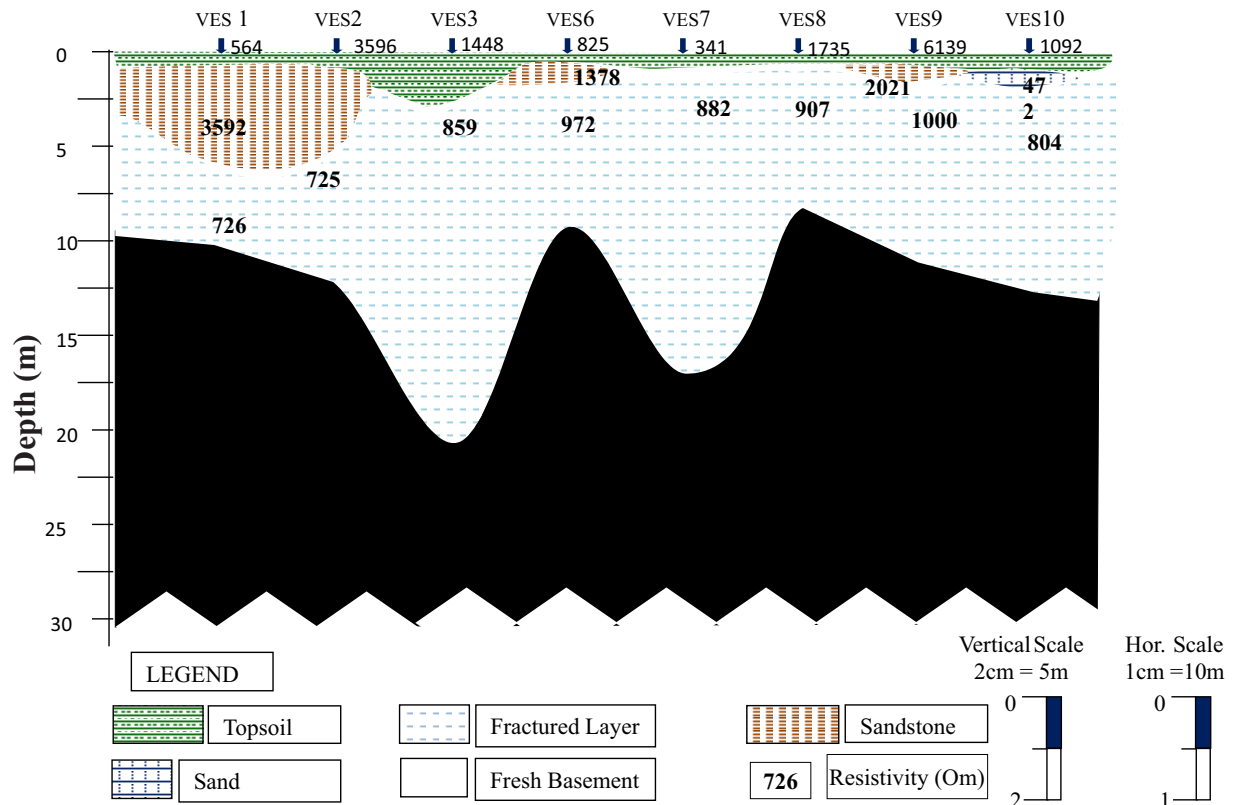


Figure 12: Geoelectric sections from VES of Kobape.

CONCLUSIONS

The aquifer mapping in Kobape was carried out using the natural electric field and electrical resistivity methods of survey. The eight traverses investigated with the NEF method showed peak frequency amplitudes of 36.6, 4.9, 0.3, 0.4, 8.5, 1.8, 9.1, and 3.6 mV respectively. The regions that have the prospect for groundwater exploration are revealed by frequency spikes on traverse 2 at station 18, 80 m below the surface, traverse 4 at station 0 at a depth between 100 and 135 m, traverse 7 at station 13 from 75–95 m below the surface, and traverse 8 at station 11 between 50 and 65 m below the surface. The overall aquifer mapping in the complex geologic terrain that straddles the boundary of crystalline basement rocks and a sedimentary basin using an integrated technique of NEF and VES revealed various confined aquifers. The NEF significantly showed station 20 on traverse 3 has a good aquifer within a fractured zone at a depth of 15 m and the same region is verified by the result obtained at VES 3, which has a fractured layer of 19.8 m thickness. Other interpretations from VES 3, 7, and 10 revealed thin and shallow fractured zones that have an average depth of 12 m to bedrock.

CONFLICT OF INTEREST

The authors declare that there is no conflict of interest.

REFERENCES

- Abiola, O., Enikanselu, P. A., and Oladapo, M. I. (2009): Groundwater potential and aquifer protective capacity of overburden units in Ado-Ekiti, southwestern Nigeria, *International Journal of Physical Sciences*, 4 (3):120-132.
- Adeeko T.O., Ojo EO, (2015): Underground Water Distribution System in Gwagwalada Area Council Abuja, Nigeria, using Resistivity Geophysical Method, *International Journal of Scientific Research in Agricultural Sciences* 2(4):097-104.
- Afolayan, J.F., Olorunfemi, M.O., Afolabi A., (2004): Geoelectric/ Electromagnetic VLF survey for groundwater development in a basement terrain – a case study *Ife Journal of Science*, 6(1): 74-78.

- Agagu, O. K. (1985): A geological guide to bituminous sediments in Southwestern Nigeria, Unpublished Report, Department of Geology, University of Ibadan.
- Akinse, A.G. and Gbadebo, A.M. (2016): Geological Mapping of Abeokuta Metropolis, Southwestern Nigeria. *Int. Journal of Scientific and Eng. Res.*, 7(8): 979-983.
- Alabi A. A, Popoola O. I., Olurin O. T., Ogungbe A. S., Ogunkoya O. A. and Okediji S. O. (2020): Assessment of groundwater potential and quality using geophysical and physicochemical methods in the basement terrain of Southwestern, Nigeria. *Environmental Earth Sciences* (2020) 79:364 <https://doi.org/10.1007/s12665-020-09107-y>
- Areola, O. (1991): *Ecology of Natural Resources in Nigeria*, Avebury Academic Publishing Group, Aldershot, England, pp 178-196.
- Ariyo, S., and Adeyemi, G. (2012): Geo-electrical Characterization of Aquifers in the Basement Complex/ Sedimentary transition zone, Southwestern Nigeria, *International Journal of Advanced Scientific Research and Technology*, (2)1.
- Avbovbo, A.A., (1980): Basement geology in the sedimentary basins of Nigeria, *Geology*; 8 (7): 323–327, doi: [https://doi.org/10.1130/0091-7613\(1980\)8<323:BGITSB>2.0.CO;2](https://doi.org/10.1130/0091-7613(1980)8<323:BGITSB>2.0.CO;2)
- Badmus, B.S. and Olatinsu, O.B. (2010): Aquifer characteristics and groundwater recharge pattern in a typical basement complex, southwestern Nigeria. *African Journal of Environmental Science and Technology* 4(6): 328-342.
- Birch, F S. (1998): Imaging the water table by filtering self-potential profiles, *Ground Water* 36(5): 779-782
- Caby, R. (1989): Precambrians Terranes of Benin – Nigeria and Northeast Brazil and the Late Proterozoic South Atlantic fit, Geological Society America Special Paper. 230:145-158.
- Coker, J.O., Mustapha, A.O., Makinde, V., and Adesodun, J.K. (2014): Radiometric Survey to Determine the Terrestrial Gamma Radiation Levels: A Case Study of Sagamu and Abeokuta, South Western Nigeria. *International Journal of Pure and Applied Sciences and Technology* 21(1): 31-38.
- Delleur, J.W., (2006) The handbook of groundwater engineering. CRC Press LLC, ISBN 9781420006001
- Frey, Herbert, [Satellite Magnetic Models, Comprehensive Modeling of the Geomagnetic Field, NASA, Retrieved 13 October 2011.](#)
- Filimonau, V., & Barth, J. A. (2016): From Global to Local and Vice Versa: On the Importance of the 'Globalization' Agenda in Continental Groundwater Research and Policy-Making, *Environmental management*, 58 (3), 491–503, doi:10.1007/s00267-016-0722-2.
- Guru B, Karthik S, Somnath B, (2017): Frequency ratio model for groundwater potential mapping and its sustainable management in cold desert, India, *Journal of King Saud University - Science* (29)3:333-347.
- Harinath, Introduction PQWT Groundwater detector PQWT-TC Series, <http://pqwtcs.com/newsDetail.aspx?nid=3675> accessed on 20th Nov., 2020
- Heilig B., Lichtenberger J., Beggan C., 2018, Natural sources of geomagnetic field variations, CERN Report No. CERN-ACC-2018-0033; CLIC-Note-1083
- Hunan, P. (2017): Development History and Practical application of Geophysical Prospecting Instrument for Natural Electric field, Geologic Exploration Equipment Institute, China.
- Hunan, P. (2018): The principle and research of Natural Electric geophysical prospecting instrument, Geologic Exploration Equipment Institute, China QQ: 2170844318.
- Kearey, P., Brooks, M. & Hill, I. (2002): An Introduction to geophysical exploration, 3rd edition, Blackwell Publishing
- Legchenko A, Baltassat J, Beauce A, Bernard J, (2002), Nuclear magnetic resonance as a geophysical tool for hydrogeologists, *Journal of Applied Geophysics*, 50:21–46

- Maineult, A., Bernabé, Y., and Ackerer, P. (2004): Electrical response of flow, diffusion and advection in a laboratory sand box, *Vadoze Zone Journal*, 3: 1180-1192
- Mosuro G., Bayewu O., and Oloruntola M., (2011): Geophysical investigation for groundwater exploration in Kobape via Abeokuta SW, Nigeria, 10.13140/2.1.4183.1686
- Muhammad S. J., Laila Khalid and Muhammad Z., K., (2020): Analytical Study of Environmental Impacts and Their Effects on Groundwater Hydrology, *Groundwater Hydrology*, Muhammad Salik Javaid, IntechOpen, DOI: 10.5772/intechopen.88002.
- Naudet, V and Binley, A., (2019): A review of the self-potential method applied to groundwater investigation, Department of Environmental Science, Lancaster University, <http://proceedings.dtu.dk/fedora/repository/dtu:1475/OBJ/article.pdf>, cited 24th October 2019.
- Nelson, S.A., (2015), *Earth & Environmental Sciences*, EENS 1110 Groundwater Handbook, Physical Geology Department, Tulane University
- Obaje, NG, (2009): *Geology and mineral resources of Nigeria*, Lecture Notes in Earth Sciences, Vol 120. Springer, Berlin, ISBN 978-3-540-92684-9. doi:10.1007/978-3-540-92685-6
- Oguntoko O; Aboaba A and Gbadebo T. A., (2009): Impact of Granite Quarrying on the Health of Workers and Nearby Residents in Abeokuta Ogun State, Nigeria, *Ethiopian Journal of Environmental Studies and Management*.2(1):1-11
- Oladele, S., and Odubote, O. (2017), Aquifer Mapping and Characterization in the Complex Transition Zone of Ijebu Ode, Southwestern Nigeria, *Forum geografic*, XVI(1), 49-58.
- Olayinka AI, Amidu SA, Oladunjoye MA, (2004): Use of Electromagnetic Profiling and Resistivity Sounding for Groundwater Exploration in the Crystalline Basement Area of Igbeti, Southwestern Nigerian, *Global Journal Geological Sciences* 2(2) 243-253
- Omatsola, M., and Adegoke, O. (1981): Tectonic evolution and Cretaceous stratigraphy of the Dahomey Basin, *Journal of Mining and Geology*, 181, 130-137
- Onoja S.O, and Osifila A.J, (2015): Integrated Geophysical Investigation of a Suspected Spring in Igbokoran, Ikare-Akoko, Southwestern Nigeria, *IOSR Journal of Applied Geology and Geophysics*, 3(5)1:83-91
- Oyegoke, S. O., Ayeni, O. O., Olowe, K. O., Adebajo, A. S., and Fayomi, O. O., (2020): Effectiveness of geophysical assessment of boreholes drilled in basement complex terrain at Afe Babalola University, using Electromagnetic (E.M.) method, *Nigerian Journal of Technology*, Vol. 39, No. 1, January 2020, pp. 36–41
- Parasnis D., (1997): *Principle of Applied Geophysics*, London: Chapman & Hall., p.275.
- Rahman, M. (1989): *Review of the Basement Geology of Southwest. Nigeria*, *Geol. Nigeria*, 943-959.
- Ranganai, R. T., Tafila, O., Baleseng, G., Montshiwa, B., (2018): Integrating Geophysical Methods to Decipher hydrogeological characteristics of a Groundwater borehole site in the University of Botswana Gaborone Campus: Critical Lessons Learnt, ISSN No.: 2664-5556 - Ubrisa - University of Botswana.
- Rensburg, R.V., (2019) AT Receiver Pseudo Science or a method worth investigating, Geotron System, Potchefstroom, South Africa, <https://gwd.org.za/wp-content/uploads/2020/06/1ATRVrprint-2-page.pdf>
- Sharma, S.P., Baranwal, V.C. (2005): Delineation of groundwater-bearing fracture zones in a hard rock area integrating very low frequency electromagnetic and resistivity data, *Journal of Applied Geophysics* 57(2): 155-166.
- Van der Velpen, B.P.A. (2004): WINRESIST Version 1.0 Resistivity Depth Sounding interpretation software. MSc Research Project, ITC, Delft, the Netherland

- Waff H. (2000), Electrical Resistivity Imaging of Groundwater Systems using Natural and Controlled Source Magnetotellurics, University of Oregon, Oregon, pp20
- William m. Alley, Richard w. Healy, James W. Labaugh, Thomas e. Reilly, (2002): Flow and Storage in Groundwater Systems, *SCIENCE*, 296(5575):1985-1990.
- Wright, E. P., (1992): The hydrogeology of crystalline basement aquifers in Africa, Geological Society, London, Special Publications, 66:1-27.
- Zonge, K.L., and Hughes, L.J., (1991) Electromagnetic Methods in Applied Geophysics: Volume 2, Application, Parts A and B, Society of Exploration Geophysicists, 713-810.